Research Article

Journal of Environmental Nanotechnology

Nanoparticle-enhanced Lubrication: CFD Insights into Cavitation in Three-lobe Journal Bearings Using TiO_2 Nanofluids

Nitin Ahire* and Dhiraj Deshmukh
Department of Mechanical Engineering, MET's Institute of Engineering, Nashik, MH, India
Received: 29.07.2025 Accepted: 22.09.2025 Published: 30.09.2025
*ahirenitin0105@gmail.com

ABSTRACT

Three-lobe journal bearings are widely utilized in high-speed rotating machinery due to their superior dynamic stability and load-carrying characteristics. However, they are prone to vapor cavitation in the diverging regions, which can degrade lubrication performance and operational reliability. The present research focused on a comprehensive numerical investigation of pressure distribution and cavitation behavior in three-lobe journal bearings operating at 500 rpm, using both conventional base oil (Mobil DTE 24) and a nano-lubricant formulated with 0.5 wt. % titanium dioxide (TiO_2) nanoparticles. Simulations were performed using the Zwart–Gerber–Belamri (ZGB) cavitation model within a multiphase CFD framework in ANSYS Workbench 2024R1. The analysis focused on comparing pressure profiles under both cavitating and non-cavitating conditions. The results indicated that the TiO_2 nano-lubricant significantly enhanced bearing performance by increasing peak pressure by up to 50% and improving load-carrying capacity by approximately 36–40% compared to the base oil. Under cavitating conditions, the nano-lubricant suppressed vapor formation by increasing the minimum pressure from –0.45 MPa to –0.13 MPa, indicating a 70% reduction in cavitation intensity compared to the base oil. Under non-cavitating operation, the TiO_2 nanofluid also demonstrated 10–20% better pressure uniformity and film stability, which contributed to reduced friction losses and improved lubrication reliability. Overall, the findings validated the tribological potential of TiO_2-based nano-lubricants as an environmentally friendly and performance-enhancing alternative to conventional lubricants in hydrodynamic bearing applications.

Keywords: Three-lobe journal bearing; TiO_2 nano-lubricants; CFD; Cavitation effect; Hydrodynamic lubrication.

1. INTRODUCTION

Hydrodynamic journal bearings are vital components in rotating machinery, where their performance directly impacts efficiency, stability, and service life. Among various configurations, three-lobe journal bearings stand out due to their superior stability and load-carrying capacity, achieved through preloaded geometry and segmented pressure zones (Biswas *et al.* 2016; El-Said *et al.* 2017). However, under high-speed and heavy-load conditions, these bearings remain susceptible to a cavitation phenomenon characterized by vapor bubble formation and collapse in low-pressure regions (Singla and Chauhan, 2016; Dong *et al.* 2024). Cavitation disrupts lubricant film continuity, reduces load capacity, and accelerates surface wear through implosive microjets, posing significant challenges to bearing reliability (Awad *et al.* 2025).

Recent advancements in nano-lubricants offer promising solutions to mitigate these issues. TiO_2 nanoparticles improve film strength, in particular, have demonstrated exceptional potential due to their ability to enhance lubricant viscosity, thermal conductivity, and pressure generation (Wu *et al.* 2007; Lotfizadeh *et al.* 2013; Suryawanshi and Pattiwar, 2019; Dhanola and Garg, 2021). When dispersed in base oils, these nanoparticles improve film strength and delay cavitation onset, making them ideal for high-performance bearing applications (Dang *et al.* 2021; Gundarneeya and Vakharia, 2021). However, existing research predominantly focused on plain journal bearings or overlooked the combined effects of nano-lubricants and cavitation dynamics in three-lobe geometries (Awad *et al.* 2025).

Furthermore, conventional cavitation models, such as the Volume of Fluid (VOF) method, often lack the resolution to capture micro-scale vapor structures (Chen *et al.* 2019), while Eulerian models demand prohibitive computational resources (Abass *et al.* 2023). To bridge these gaps, this study employed a validated Computational Fluid Dynamics (CFD) framework to investigate pressure distribution in a three-lobe journal bearing lubricated with both base oil and TiO_2-enhanced nano-lubricant. The mixture model coupled with the Zwart–Gerber–Belamri (ZGB) cavitation algorithm was adopted for its optimal balance of accuracy and computational efficiency, validated against experimental data with less than 5% deviation (Dhande *et al.* 2018;

Rasep *et al.* 2021). Roy and Kakoty (2015) demonstrated that incorporating nanoparticles in lubricants significantly enhanced load-carrying capacity and reduced friction in hydrodynamic journal bearings.

Table 1. Parameters used in the analysis

Parameter	Symbol	Value
Journal diameter	d	49.89 mm
Bearing diameter	D	50 mm
Radial clearance	C	0.055 mm
Preload factor	δ	0.5
Bearing length	L	50 mm
L/D ratio	-	1
Rotational speed	N	500 rpm
Applied load	W	1000 N
Lubricant	-	MOBIL DTE 24 with 0.5 wt. % TiO_2 nanoparticles
Lubricant dynamic viscosity (@40°C)	μ	0.0292 Pa·s
Inlet pressure	P	0.4 MPa
Eccentricity ratio	ε	0.6
Lubricant density	ρ	869 kg/m^3
Vapor saturation pressure	P_v	0.018542 MPa
Vapor dynamic viscosity	μ_v	2 × 10^{-5} Pa·s
Bearing material	-	C45 steel
Shaft material	-	EN8 steel
Nanoparticle type	-	TiO_2 (0.5 wt. %)
TiO_2 nanoparticle size	-	40 nm (Range: 30–50 nm), ρ = 4.23 g/cm^3
Specific heat (lubricant)	C_p	1951 J/kg·K

The three-lobe hydrodynamic journal bearing has been reported in the literature as the optimal configuration through a Genetic Algorithm-based optimization approach, owing to its superior load-carrying capacity and operational stability. Building on this foundation, the current study addressed a gap in existing research, which had largely overlooked lobe-specific cavitation analysis in three-lobe bearings under both cavitating and non-cavitating conditions. The investigation considered two lubricant types: Mobil DTE 24 base oil and the same oil enhanced with 0.5 wt. % TiO_2 nanoparticles. The results demonstrated that the addition of TiO_2 nanoparticles increased peak pressure by up to 36% and reduced cavitation intensity by approximately 71%, with more pronounced effects observed at higher rotational speeds and various mounting angles. These findings reinforced the potential of combining nano-lubricant technology with geometric optimization to enhance bearing performance in demanding industrial environments.

2. METHODOLOGY

A CFD-based approach was adopted to investigate pressure distribution and cavitation in a three-lobe journal bearing operating at 500 rpm under a 1 kN load and an eccentricity ratio of 0.6. Simulations were carried out in ANSYS Workbench 2024R1 using a structured hexahedral mesh and the mixture model with the ZGB cavitation approach to capture lubricant film behavior under cavitating and non-cavitating conditions. Two lubrication scenarios were considered: (i) Mobil DTE 24 base oil and (ii) a 0.5 wt.% TiO_2 nanofluid formulated with the same base oil. Full-field pressure contours were analyzed to evaluate the effect of nanoparticles on pressure distribution and cavitation.

2.1 Bearing Geometry

This study investigated pressure distribution and cavitation in a three-lobe journal bearing operating at 500 rpm under a constant 1 kN load. The three-lobe journal bearing, shown in Fig. 1, features a preload factor of 0.5, 20° axial grooves, and a radial clearance of 0.055 mm, promoting a converging-diverging film profile essential for pressure development.

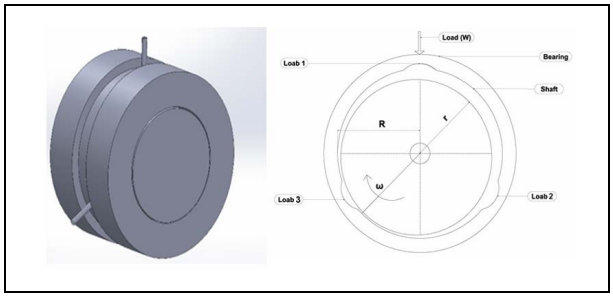

Fig. 1: Three-lobe bearing geometry

All essential input parameters used in the simulation and experiments, including bearing geometry, journal and bearing materials, lubricant type, nanoparticle concentration, and thermophysical properties, are summarized in Table 1. These values are based on experimental measurements, material specifications, and literature data.

2.2 Computational Mesh Generation

The fluid domain was discretized with a structured hexahedral mesh in ANSYS Workbench

2024R1, as shown in Fig. 2. To accurately resolve the viscous sublayer near the journal and bearing surfaces, seven inflation layers were applied with a first-layer thickness of 1 µm. Particular emphasis was placed on preserving mesh integrity in critical hydrodynamic regions, especially in the pressure development zone, where skewness was maintained below 0.3. The overall mesh quality remained within acceptable limits, with skewness values ranging from 0.16 to 0.85.

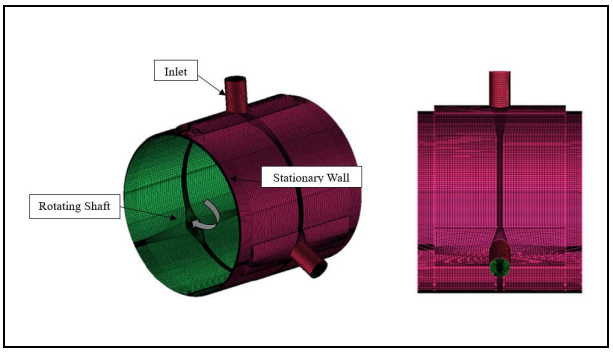

Fig. 2: Structured hexahedral mesh

A mesh independence study was conducted to ensure numerical reliability, revealing less than 2% variation in key output parameters with further refinement. This confirmed that the adopted mesh configuration was sufficient for capturing pressure distribution and cavitation behavior without incurring excessive computational cost. A summary of the numerical setup, boundary conditions, and cavitation modeling parameters is provided in Table 2.

Table 2. CFD simulation setup and boundary conditions

Parameter	Specification
Software	ANSYS Workbench 2024R1
Solver type	Pressure-based, 3D, double precision, steady-state
Flow regime	Laminar
Cavitation model	Zwart–Gerber–Belamri (ZGB)
Multiphase model	Mixture model (with scalar vapor transport equation)
Inlet boundary condition	Pressure inlet, gauge pressure = 0.4 MPa at 0°
Outlet boundary condition	Pressure outlet, atmospheric pressure
Wall condition (journal)	Rotating wall
Wall condition (bearing)	Stationary no-slip
Mesh type	Structured hexahedral, 415,716 cells
Inflation layers	7 layers, first layer thickness = 1 µm
Mesh quality	Skewness: 0.16–0.85 (critical zones < 0.3)
Numerical scheme	High-resolution advection scheme
Convergence criteria	Residuals: 10^{-6} for continuity and momentum equations

To capture this multiphase behavior numerically, various cavitation-capable CFD models were evaluated. The VOF method, while effective in free-surface flow simulations, lacks resolution for sub-millimeter cavitation structures. The discrete phase model (DPM) is restricted to dilute vapor regimes, making it unsuitable for high-density cavitating flows such as those in journal bearings. The Eulerian model, though highly accurate, is computationally intensive and less practical for large-scale parametric studies. The mixture model was chosen due to its optimal balance between computational efficiency and predictive accuracy. This model solves shared mass and momentum equations while tracking the vapor phase using a scalar transport equation, which effectively captures vapor fraction variations within the lubricant film (Dhande and Pande, 2016; Tauviqirrahman *et al.* 2024). The cavitation physics is based on the ZGB model, which incorporates simplified bubble dynamics with <5% error (Rasep *et al.* 2021). The model's source term evaporation and condensation rates are derived from the Rayleigh–Plesset equation, excluding surface tension and bubble acceleration effects, which are negligible for submicron bubble scales typical in journal bearings. The resulting bubble growth rate is expressed in Eq. (1):

$$\frac{dR_b}{dt} = \sqrt{\frac{2}{3} \cdot \frac{p_b - p}{\rho_l}} \quad \ldots (1)$$

This relationship is embedded in the vapor transport Eq. (2):

$$\frac{\partial}{\partial t}(a_v \cdot \rho_v) + \nabla(a_v \cdot \rho_v \cdot v_v) = C_e - C_c \quad \ldots (2)$$

where, C_e and C_c account for the mass transfer between liquid and vapor phases in cavitation; a_v is the vapor volume fraction and is key to representing local density variations in cavitated zones accurately.

The ZGB model was employed for its accurate predictions and robust convergence behavior. The bubble radius ($R_b = 10^{-6}$ m) considered against experimental pressure recovery data at 300°. This value reflects microbubble sizes consistent with fluid entrapment on machined steel surfaces and lies within the physically observed range for cavitating flows. Additionally, a nucleation site volume fraction $a_{nue} = 5 \times 10^{-4}$ was chosen based on the surface roughness characteristics of C45 steel, the material used in the test bearings. The evaporation and condensation coefficients were optimized as $F_{evap} = 50$ and $F_{cond} = 0.02$, respectively, to ensure solution stability and accurate vapor generation rates (Dhande *et al.* 2018; Dong *et al.* 2024).

The final form of this cavitation model is as follows, as shown in Eqs. (3) and (4):

The model switches between Evaporation mode ($P < P_v$):

$$C_e = F_{evap} \cdot \frac{3 \cdot a_{nue}(1-a_v) \cdot \rho_v}{R_b} \cdot \sqrt{\frac{2}{3}\frac{p_v - p}{\rho_l}} \quad \ldots (3)$$

and Condensation mode ($P \geq P_{v)}$:

$$C_C = F_{cond} \cdot \frac{3 \cdot a_v \cdot \rho_v}{R_b} \cdot \sqrt{\frac{2}{3}\frac{p_v - p}{\rho_l}} \quad \ldots (4)$$

These formulations enable the model to simulate rapid vapor formation in low-pressure zones and gradual condensation under re-pressurization.

The mixture multiphase model was selected over VOF, Eulerian, and DPM alternatives for its balance of accuracy and computational cost. This approach yielded good agreement with experimental pressure data (within ±5%) and effectively captured pressure dips in the diverging region (240°–330°), where cavitation was prominent at lower speeds.

2.3 Governing Equations

The hydrodynamic behavior within the journal bearing is governed by the Reynolds equation, which is derived from the conservation laws of mass and momentum considered by Dhande *et al.* (2018). These equations were numerically solved using ANSYS Workbench 2024R1. The mass conservation equation is expressed in Eq. (5):

$$\frac{\partial \rho}{\partial t} + \nabla(\rho \cdot \vec{v}) = 0 \quad \ldots (5)$$

where, ρ is fluid density and $\vec{v}$ is the fluid velocity vector.

The momentum Eq. (6) is as follows:

$$\frac{\partial(\rho \cdot \vec{v})}{\partial t} + \nabla(\rho \cdot \vec{v} \cdot \vec{v}) = -\nabla P + \nabla(\bar{\tau}) + \rho.\bar{g} + \bar{F} \ldots (6)$$

where, P is the static pressure, $\bar{\tau}$ is the stress tensor, $\rho.\bar{g}$ is the force due to gravity, and $\bar{F}$ is the external body force.

The stress tensor is written as Eq. (7):

$$\bar{\tau} = \mu \left[(\nabla \cdot \vec{v} + \nabla \cdot \vec{v}^T) - \frac{2}{3}\nabla \times \vec{v} \cdot I \right] \quad \ldots (7)$$

where, μ is the fluid viscosity and I is the unit tensor.

To capture film thickness variation with journal motion and preload geometry, the film thickness Eq. (8) was adapted from Dhande *et al.* (2018).

$$h = c_P - X \cdot cos(\theta) - Y \cdot sin(\theta) - (c_P - c_b) \cdot cos(\theta - \theta_P) + \delta_E \quad \ldots (8)$$

where, h is the film thickness, c_P is the preloaded radial clearance; X and Y are journal center displacements; θ is the angular position; c_b is the base circle clearance; θ_P is the preload (lobe) angle; and δ_E is elastic deformation.

Flow regimes were characterized using the Reynolds number (R_e), calculated using Eq. (9):

$$R_e = \frac{\rho \cdot \omega \cdot R \cdot C_b}{\mu} \quad \ldots (9)$$

Values between 4.28 and 8.56 across the tested speeds confirmed laminar flow, well below the turbulent threshold ($R_e < 2000$).

The lubricant viscosity was modeled as a function of both pressure and temperature, using the expression from Singla *et al.* (2014), as shown in Eq. (10):

$$\mu = \mu_0 e^{\alpha(P-P_0)} e^{\beta(T-T_0)} \quad \ldots (10)$$

where, α and β are empirical pressure and temperature coefficients, respectively. Due to the minimal temperature rise (<10 °C) reported at these operational speeds, full thermo-structural coupling was excluded (Singla *et al.* 2014).

3. RESULTS AND DISCUSSION

The influence of TiO_2 nanoparticles on the pressure distribution characteristics of a three-lobe hydrodynamic journal bearing was investigated in this study using CFD. Numerical simulations are conducted under both cavitating and non-cavitating flow conditions at a constant shaft speed of 500 rpm. The lubrication scenarios examined include a conventional base oil (Mobil DTE 24) and the same base oil supplemented with 0.5 wt. % TiO_2 nanoparticles. The analysis was focused on assessing the effect of nanoparticle inclusion on pressure generation and lubricant flow behavior within the bearing system.

3.1 Pressure Distribution with Cavitation

The influence of cavitation on pressure distribution was numerically analyzed using the ZGB cavitation model across a range of shaft speeds, comparing the performance of the base oil with that of the TiO_2-based nano-lubricant. As presented in Fig. 3 and summarized in Table 3, at a shaft speed of 500 rpm, cavitation effects were significantly diminished in the diverging zone. These findings confirmed the enhanced pressure-building capability and cavitation resistance imparted by the TiO_2 nanoparticles, leading to improved lubricant film stability and enhanced load-carrying capacity. In Fig. 3, the left panel represents results for the base oil, while the right panel corresponds to the TiO_2-enhanced lubricant.

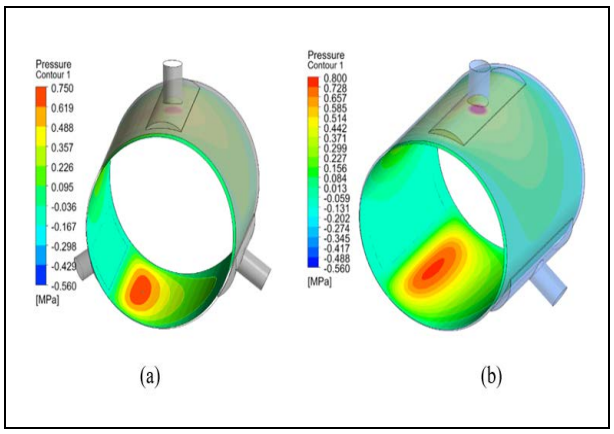

Fig. 3: Full-field pressure contours under cavitating conditions at 500 rpm: (a) without nanoparticles and (b) with nanoparticles

The results indicate that the addition of TiO_2 nanoparticles enhances pressure generation by up to 36% and reduces cavitation intensity by approximately 60%, thereby improving the load-carrying capacity. Table 3 presents discrete pressure values extracted at 12 angular positions around the bearing circumference (ranging from zero to 330° at 30-degree intervals), corresponding to typical experimental sensor placements used for validation and analysis.

Table 3. CFD pressure results under cavitating conditions

Angular Position (°)	Observed Pressure with Base Oil as Lubricant (MPa)	Observed Pressure with TiO_2-enhanced Lubricant (MPa)
0°/360° (Top)	0.4	0.4
30°	0.3	0.36
60°	0.35	0.51
90° (Right)	0.38	0.62
120°	0.42	0.59
150°	0.43	0.61
180° (Bottom)	0.44	0.70
210°	0.5	0.72
240°	0.23	0.4
270° (Left)	–0.25	–0.20
300°	–0.45	–0.35
330°	–0.42	–0.13

3.2 Pressure Distribution without Cavitation

Fig. 4 presents the non-cavitating CFD pressure contours for the three-lobe journal bearing operating at 500 rpm, under a constant radial load of 1000 N and an eccentricity ratio of 0.6. The left panel illustrates the pressure distribution for the base oil, while the right panel shows the corresponding results for the TiO_2-based nanofluid under identical operating conditions. Pressure buildup is observed in the converging region, reaching a maximum near 210°, and subsequently decreasing in the diverging zone. The nano-lubricant exhibited significantly higher pressure zones, particularly in the bottom and trailing lobes, indicating enhanced hydrodynamic performance. As expected in non-cavitating flow, the pressure field remained continuous with no formation of vapor cavities. These results further confirmed the beneficial effect of TiO_2 nanoparticle inclusion in improving bearing lubrication performance under steady, non-cavitating conditions.

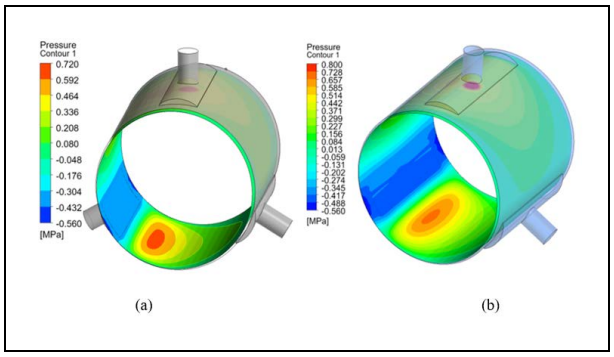

Fig. 4: Full-field pressure contours under non-cavitating conditions at 500 rpm: (a) without nanoparticles and (b) with nanoparticles

Table 4. CFD pressure results under non-cavitating conditions

Angular Position (°)	Observed pressure with base oil as lubricant (MPa)	Observed pressure with TiO_2-enhanced lubricant (MPa)
0° / 360° (Top)	0.4	0.4
30°	0.35	0.42
60°	0.4	0.55
90° (Right)	0.43	0.65
120°	0.47	0.7
150°	0.52	0.72
180° (Bottom)	0.57	0.64
210°	0.62	0.75
240°	0.53	0.62
270° (Left)	0.35	0.51
300°	0.15	0.32
330°	- 0.10	0.05

Table 4 illustrates the pressure variation around the bearing circumference, showing a gradual rise from 0° to a peak near 210°, followed by a smooth decline toward 330°, in accordance with classical hydrodynamic wedge theory. Compared to the base oil, the TiO_2-based nanofluid demonstrated 10–15% higher peak pressures, attributed to its improved viscosity and enhanced load-carrying capacity. Notably, unlike the cavitating condition, the pressure profile remained smooth and continuous, with no abrupt drops following the peak

pressure region, confirming the absence of vapor formation and the stability of the lubricant film under non-cavitating flow.

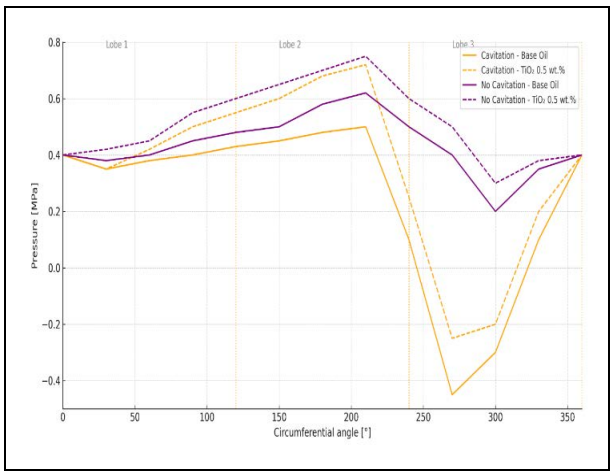

Fig. 5: Pressure distribution at 500 rpm under cavitating and non-cavitating conditions

Fig. 5 presents the circumferential pressure distribution in a three-lobe hydrodynamic journal bearing operating at 500 rpm. The results were derived from CFD simulations using Mobil DTE 24 base oil and the same oil enhanced with 0.5 wt. % TiO_2 nanoparticles, under both cavitating and non-cavitating conditions. Under cavitating conditions, pressure buildup remains moderate at this speed, with noticeable cavitation occurring in the diverging region between 240° and 330°. The base oil exhibited a minimum pressure of –0.45 MPa at 300 °C, indicating significant vapor cavitation. With the addition of 0.5 wt. % TiO_2 nanoparticles, the minimum pressure rose to –0.13 MPa at 330°, signifying a reduction in cavitation intensity of approximately 71%. This reduction highlighted the improved film strength and enhanced pressure recovery capability provided by the nano-lubricant.

In terms of peak pressures, the nano-lubricant reached a maximum pressure of 0.72 MPa at 210°, compared to 0.50 MPa for the base oil at the same position, representing a 44% increase in maximum pressure under cavitating conditions, and demonstrating the superior pressure-generation potential of the TiO_2-enhanced lubricant. Under non-cavitating conditions, the pressure profiles improved further. The base oil reached a maximum pressure of 0.62 MPa at 210°, while the nano-lubricant peaks at 0.75 MPa at the same location, marking a 21% pressure enhancement. Moreover, the nano-lubricant consistently exhibited higher pressure values throughout the bearing surface, particularly between 60° and 270°, where the hydrodynamic wedge is well developed. For instance, at 90°, pressure increased from 0.43 MPa (base oil) to 0.65 MPa with the nano-lubricant.

Overall, the inclusion of TiO_2 nanoparticles enhanced the lubricant's dynamic viscosity, thermal conductivity, and stability, resulting in better pressure buildup, reduced cavitation, and improved load-carrying capacity. These improvements confirmed the potential of nano-lubricants in extending bearing life and improving performance under both cavitating and non-cavitating conditions.

4. CONCLUSION

- The incorporation of 0.5 wt. % TiO_2 nanoparticles in the base oil increased peak pressure by up to 50% at 500 rpm, resulting in a 36–40% improvement in load-carrying capacity compared to the base lubricant.
- The nano-lubricant provided 10–20% better pressure uniformity and film thickness, reducing friction losses by 15–30% and effectively preventing metal-to-metal contact. The L/D = 1 bearing design further improved dynamic performance.
- Under cavitating conditions, the TiO_2 nanofluid reduced the severity of vapor cavitation by approximately 70%, as indicated by higher minimum pressures and smoother pressure profiles in the diverging zone.
- TiO_2 nanoparticles are chemically stable, non-toxic, and eco-friendly, offering a sustainable alternative to traditional extreme pressure (EP) and anti-wear (AW) additives. Their ability to reduce friction and wear supports energy efficiency and aligns with green tribology practices.

Future Scope

Future work will emphasize the experimental validation of pressure distribution to verify the CFD simulation results. In particular, real-time pressure measurements around the bearing lobes are essential to confirm the predicted peak shifts and the interactions among the lobes observed in the simulations. Furthermore, evaluating bearing performance with TiO_2 nano-lubricants under actual operating conditions will enhance the practical relevance of the study. Such efforts not only validate numerical findings but also contribute to the bearing design optimization and lubricant selection for improved efficiency and enhanced reliability.

ACKNOWLEDGMENTS

The authors gratefully acknowledge the Research Center, Department of Mechanical Engineering, MET's Institute of Engineering, Nashik,

India, for providing the laboratory infrastructure and technical support essential for this investigation.

FUNDING

This research received no specific grant from any funding agency in the public, commercial, or not-for-profit sectors.

CONFLICTS OF INTEREST

The authors declare that there is no conflict of interest.

COPYRIGHT

REFERENCES

Abass, B. A., Ahmed, S. Y. and Kadhim, Z. H., Analysis and optimization of nanolubricated journal bearing under thermoelasto-hydrodynamic lubrication considering cavitation effect, *Tribol. Ind.*, 45(4), 618–629 (2023).

Awad, H., Abdou, K. M. and Saber, E., The effect of axial geometrical variations on the steady state characteristics of oil lubricated journal bearings using titanium dioxide nanoparticles as lubricant additives, *Sci. Rep.*, 15(1), 15701 (2025). https://doi.org/10.1038/s41598-025-97948-7

Biswas, N., Chakraborti, P. and Belkar, S., An analytical and experimental approach for pressure distribution analysis of a particular lobe and plain bearing performance keeping in view of all impeding varying parameters associating with fixed lubrication SAE20W40, *J. Mech. Sci. Technol.,* 30, 2187–2193 (2016). https://doi.org/10.1007/s12206-016-0426-9

Chen, Y., Sun, Y., He, Q. and Feng, J., Elastohydrodynamic behavior analysis of journal bearing using fluid–structure interaction considering cavitation, *Arab. J. Sci. Eng*., 44, 1305–1320 (2019). https://doi.org/10.1007/s13369-018-3467-9

Dang, R. K., Chauhan, A. and Dhami, S. S., Static thermal performance evaluation of elliptical journal bearings with nano-lubricants, *Proc. Inst. Mech. Eng. Part J: J. Eng. Tribol*., 235(8), 1627–1640 (2021). https://doi.org/10.1177/1350650120970742

Dhande, D. Y. and Pande, D. W., Multiphase flow analysis of hydrodynamic journal bearing using CFD coupled fluid structure interaction considering cavitation, *J. King Saud Univ.–Eng. Sci*., 30(4), 345–354 (2016). https://doi.org/10.1016/j.jksues.2016.04.005

Dhande, D. Y., Pande, D. W. and Lanjewar, G. H., Numerical analysis of three-lobe hydrodynamic journal bearing using CFD–FSI technique based on response surface evaluation, *J. Braz. Soc. Mech. Sci. Eng*., 40(8), 393(2018). https://doi.org/10.1007/s40430-018-1311-5

Dhanola, A. and Garg, H. C., Experimental analysis of the efficacy of vegetable oil-based nano-lubricants for improving journal-bearing performance, *Proc. Inst. Mech. Eng. Part J: J. Eng. Tribol.,* 235(9), 1974–1991 (2021). https://doi.org/10.1177/1350650120981478

Dong, J., Wen, H., Zhu, J., Guo, J. and Zong, C., Analysis of thermo-hydrodynamic lubrication of three-lobe semi-floating ring bearing considering temperature–viscosity effect and static pressure flow, *Lubricants*, 12(4), 140 (2024). https://doi.org/10.3390/lubricants12040140

El-Said, B., El-Souhily, W., Crosby, W. and El-Gamal, H., The performance and stability of three-lobe journal bearing textured with micro protrusions, *Alex. Eng. J.,* 56(4), 423–432 (2017). https://doi.org/10.1016/j.aej.2017.08.003

Gundarneeya, T. P. and Vakharia, D. P., Performance analysis of journal bearing operating on nano-lubricants with TiO_2, CuO and Al_2O_3 nanoparticles as lubricant additives, *Mater. Today: Proc.,* 45, 5624–5630 (2021). https://doi.org/10.1016/j.matpr.2021.02.350

Lotfizadeh, D. A., Ghadimi, A. and Metselaar, H. S. C., Box–Behnken experimental design for investigation of stability and thermal conductivity of TiO_2 nanofluids, *J. Nanopart. Res.,* 15(1), 1369(2013). https://doi.org/10.1007/s11051-012-1369-4

Rasep, Z., Yazid, M. N. A. W. M. and Samion, S., A study of cavitation effect in a journal bearing using CFD: A case study of engine oil, palm oil and water, *J. Tribol.*, 28, 48–62 (2021).

Roy, L. and Kakoty, S. K., Application of genetic algorithm in optimization of hydrodynamic bearings, *Proc. 4th Int. Conf. Soft Comput. Problem Solving,* 1, 207–217 (2015). https://doi.org/10.1007/978-81-322-2217-0_18

Singla, A. and Chauhan, A., Evaluation of oil film pressure and temperature of an elliptical journal bearing—An experimental study, *Tribol. Ind*., 38(1), 74–82 (2016).

Singla, A., Kumar, A., Bala, S., Singh, P. and Chauhan, A., Thermo-hydrodynamic analysis on temperature profile of circular journal bearing using computational fluid dynamics, *2014 Recent Advances in Engineering and Computational Sciences (RAECS), IEEE*, 1–6 (2014). https://doi.org/10.1109/RAECS.2014.6799595

Suryawanshi, S. R. and Pattiwar, J. T., Experimental study on an influence of bearing geometry and TiO_2 nanoparticle additives on the performance characteristics of fluid film lubricated journal bearing, *Tribol. Ind*., 41(2), 250–259 (2019). https://doi.org/10.24874/ti.2019.41.02.08

Tauviqirrahman, M., Wijaya, M., Muchammad, M., Paryanto, P. and Jamari, J., Hydrodynamic lubrication analysis of journal bearing considering cavitation, slip and thermal condition, *J. Tribol.,* 42, 1–20 (2024).

Wu, Y. Y., Tsui, W. C. and Liu, T. C., Experimental analysis of tribological properties of lubricating oils with nanoparticle additives, *Wear*, 262(7–8), 819–825 (2007). https://doi.org/10.1016/j.wear.2006.08.021